

Multiphase Reacting Flow Modeling of Singlet Oxygen Generators for Chemical Oxygen Iodine Lasers

Lawrence C. Musson^a, Roger P. Pawlowski^a, Andrew G. Salinger^a,
Timothy J. Madden^b and Kevin B. Hewett^b

^aSandia National Laboratories, Center for Computation, Computers, Information, and Mathematics,
Albuquerque, NM, USA

^bAir Force Research Laboratory, Directed Energy Directorate, Kirtland Air Force Base, NM, USA

ABSTRACT

Singlet oxygen generators are multiphase flow chemical reactors that produce energetic oxygen to be used as a fuel for chemical oxygen iodine lasers. In this paper, a theoretical model of the generator is presented that consists of a two-phase reacting flow model that treats both the gas phase and dispersed (liquid droplet) phase. The model includes the discretization over droplet size distribution as well. Algorithms for the robust solution of the large set of coupled, nonlinear, partial differential equations enable the investigation of a wide range of operating conditions and even geometric design choices.

Keywords: Singlet Oxygen generator, chemical oxygen iodine laser, sog, coil, multiphase, gfem, reacting flow

1. INTRODUCTION

The singlet oxygen generator (SOG) is a low-pressure, multiphase flow chemical reactor that is used to produce molecular oxygen in an electronically excited state, i.e. singlet delta oxygen. The primary product of the reactor, the energetic oxygen, can be used to dissociate and energize iodine. The gas mixture including the iodine can be accelerated to a supersonic speed and lased. Thus the SOG is the fuel generator for the chemical oxygen iodine laser (COIL). The COIL, Figure 1, has important application for both military purposes—it was developed by the US Air Force in the 1970s—and, as the infrared beam is readily absorbed by metals, industrial cutting and drilling.

The SOG appears in various configurations, but the one in focus here is a crossflow SOG. A gas consisting of molecular chlorine and a diluent, usually helium, is pumped through a roughly rectangular channel. An aqueous solution of hydrogen peroxide and potassium hydroxide is pumped through small holes into the channel, perpendicular to the direction of the gas flow, causing the solution to become aerosolized. In the liquid droplets, dissociation of the potassium hydroxide draws a proton from the hydrogen peroxide to generate an HO_2^- radical. When Chlorine diffuses from the gas phase into the liquid, it reacts with the HO_2^- ion to produce the singlet delta oxygen; some of the oxygen diffuses back into the gas phase for use in the next stage of the COIL.

The focus of this work is to generate a predictive multiphase flow model of the SOG which can then aid in optimizing its design. What follows is a description of the model that we have employed, the solution method, and sample results.

2. MODEL EQUATIONS

The model that was chosen is the Eulerian-Eulerian form of the multiphase flow, isothermal Navier-Stokes equations wherein one set of the equations represents the gas phase and another equation set represents the liquid phase. As flows in the SOG are dominated by advection, a stabilized Galerkin finite element formulation is employed to solve the partial differential equations. The set of equations is large, even for the 2D models studied here. Thus we are taking advantage of and developing algorithms to harness the power of large parallel computing architectures to solve the steady-state form of these equations rapidly, which enables the exploration the large parameter space of the equations *via* continuation methods. For a complete description of the equations and solution methods see Shadid *et al.*¹ and Musson *et al.*²

Further author information: (Send correspondence to Lawrence C. Musson)

Lawrence C Musson.: E-mail: lcmusso@sandia.gov

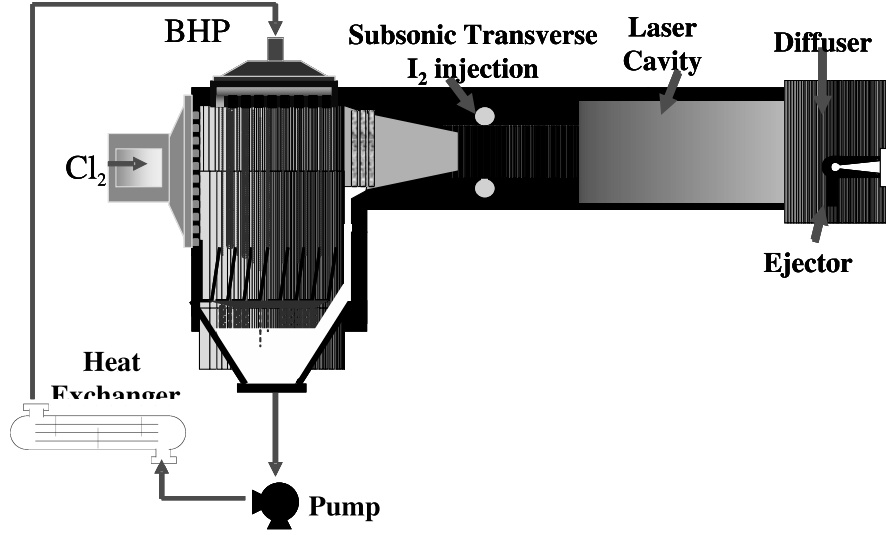


Figure 1. Schematic of a typical chemical oxygen iodine laser. The initial stage is the singlet oxygen generator. Subsequent stages are mixing, supersonic nozzle, lasing and exhaust.

2.1 Continuous Phase Equations

The gas phase in the singlet oxygen generator is the continuous phase. In this model, the gas flow is assumed to be steady and incompressible. The appropriate continuum equation set for such a system is the steady form of the Navier-Stokes equations consisting of continuity,

$$\nabla \cdot \mathbf{v} = 0 \quad (1)$$

and momentum conservation,

$$\rho \mathbf{v} \cdot \nabla \mathbf{v} = \nabla \cdot \mathbf{T} + \mathbf{s}. \quad (2)$$

\mathbf{T} is the Cauchy stress tensor of a Newtonian fluid:

$$\mathbf{T} = -p\mathbf{I} + \mu(\nabla \mathbf{v} + \nabla \mathbf{v}^T) \quad (3)$$

where p is the isotropic hydrodynamic pressure, μ is the mixture viscosity, and \mathbf{I} is the identity tensor.

For ideal gas mixtures, the density is computed from

$$\rho = \frac{\mathcal{P}_{SOG}}{RT \sum_{j=1}^{N_{sp}} \frac{Y_j}{M_j}} \quad (4)$$

where \mathcal{P}_{SOG} is the nominal thermodynamic pressure of the reactor, R is the universal gas constant, T is the temperature, Y_j is the mass fraction of the j^{th} species, M_j is the molecular weight of the j^{th} species, and N_{sp} is the number of gas-phase species. The pressure \mathcal{P}_{SOG} is user specified.

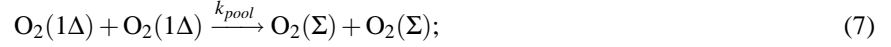
Singlet delta oxygen is produced in the reactor by chemical conversion, and so the composition of the gas phase must also be modeled. The conservation equation for gas species j includes advection, diffusion, and reaction contributions,

$$\rho \mathbf{v} \cdot \nabla Y_j + \nabla \cdot (-\rho D_{c_j} \nabla Y_j) + s_{Y_j} = 0. \quad (5)$$

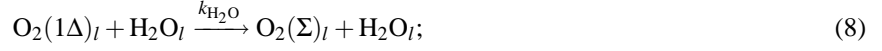
In this work, the source terms s_{Y_j} that appear in Equation 5 arise from chemical reactions. This model follows in part the one proposed by Thayer.³ Four chemical reactions in the SOG generator are modeled: (i) Singlet delta oxygen generation in the liquid phase of the basic hydrogen peroxide (BHP),



(ii) Homogeneous gas phase deactivation by a pooling reaction,



(iii) Homogeneous liquid phase quenching of the singlet delta oxygen,



and (iv) heterogeneous quenching of the singlet delta oxygen at, the droplet surface



Whereas Thayer's model predicted conversion given a field of uniform-sized droplets, this model allows a distribution of droplet sizes. The generalization of Thayer's model to a multiple of droplet sizes is described by Musson *et al.*²

2.2 Dispersed Phase Flow Modeling

The second phase is one of droplets dispersed within the gas. In the SOG, the equations model not only the spatial variation of number density, composition, and momentum of droplets, but also models the distribution of each of these quantities as a function of droplet size. A complete description of the dispersed phase flow equations is not possible in this space. A complete description is being prepared in Musson *et al.*²

When accounting for mass transfer of dispersed phase systems, the local mass density of the dispersed phase must be computed. The mass density is in general a function of four quantities: the material density, the volume of a single particle or droplet, the number density of the droplets and the composition of the phase. The material density is, for the systems considered here, a specified constant and the droplet volume is computed. The number density is a dependent variable and is solved for in the solution of the differential equation set. The composition in the droplet can also be a dependent variable when the chemical conversion is being tracked.

As will be seen in the final presentation of the equations in this section, the droplet number density is solved for directly. However, the number density is derived from a more primitive quantity called the probability density function (PDF) for the particle distribution and is a function of space, time and droplet size, *i.e.* $n = n(\mathbf{x}, t, d)$. The total number density of droplets of all sizes within a sufficiently large spatial element is related to the PDF by

$$N(\mathbf{x}, t) = \int_0^{\infty} n(\mathbf{x}, t, D) dD \quad (10)$$

where N is the number of droplets per unit volume, and D is the droplet diameter. Or, if the number density of all droplets between the size range of d_1 and d_2 is required, it is computed by

$$N(\mathbf{x}, t) = \int_{d_1}^{d_2} n(\mathbf{x}, t, D) dD. \quad (11)$$

Finite element basis functions are used to construct the field variables such as the number density, N_i , and velocity, \mathbf{v}_i , and so on, as a function of the independent variables, space and time. In dispersed phase flows, variations over droplet size is critically important as well. For convenience, a piecewise constant basis function is used to expand solutions as a function of droplet size. In this way, the mass and momentum conservation equations become sets of equations over space and time. If the entire range of droplet sizes to be modeled is subdivided into m subdomains of droplet size, then there will be m mass conservation equations in the set. Often, the subdomains of droplet size are referred to as bins.

The mass density of droplets of a particular size is

$$Q_i = \rho_l v_i N_i, \quad (12)$$

where ρ_l is the liquid density, v_i is the average volume of droplets in the diameter range of d_1 to d_2 and N_i is the number density of droplets in that same size range as computed from Equation 11. Moreover, if the composition of the droplets is also a concern, the mass density of a particular component of the droplets is

$$Q_i^k = \rho_l v_i N_i Y_k^i, \quad (13)$$

where Y_k is the mass fraction of component k in a droplet within the stated size range.

Mass conservation species j in droplets in size class i is represented by the partial differential equation

$$\nabla \cdot (\mathbf{v}_d^i \rho_l v_i N_i Y_j^i) = \nabla \cdot D \nabla (\rho_l v_i N_i Y_j^i) + s_{mass}^i, \quad (14)$$

where s_{mass}^i is a collection of source terms. in the application discussed herein, s_{mass}^i consists of two parts: a term representing mass exchange between size bins due to droplet agglomeration and a term representing mass exchange due to conversion of components within a size bin by chemical reaction, viz.

$$s_{mass}^i = s_{agg}^i + s_{conversion}^i. \quad (15)$$

The source term from conversion is

$$s_{conversion}^i = u_i N_i \quad (16)$$

where u_i is the mass change per droplet due to conversion. The exact form of u_i depends on the chemistry being modeled. The variable s_{agg} is effectively a second-order source term that is too lengthy to be described in this document. An excellent presentation of the equations employed by this model is described by Gelbard and Seinfeld.⁴

In the systems under consideration here, droplets are injected at a relatively high speed into a flow of gas, also moving at a relatively high speed, and in a direction orthogonal to the gas flow. In these systems it is imperative to account separately for the momentum transfer of the droplets. Indeed it is desirable to account for the dispersed phase momentum as a function of droplet size as smaller droplets become entrained more readily than larger ones. And so droplet velocity is represented by piecewise constant basis functions in droplet size (or classified into bins by size) in precisely the same way that number density and droplet component mass fraction were done. The momentum conservation of the dispersed phase is thus described by vector partial differential equations equal in number to the number of basis functions or bins used to represent the size distribution. The equation is

$$\rho_l v_d^i \frac{\partial \mathbf{v}_d}{\partial t} + \rho_l v^i \mathbf{v}_d^i \nabla \cdot \mathbf{v}_d^i = s_{momentum}^i \quad (17)$$

where \mathbf{v}_d^i is the velocity and v^i the volume of droplets of a size represented by bin i , $s_{momentum}^i$ is a collection of source terms that contribute to momentum transfer.

The two main contributors to $s_{momentum}^i$ arise from particle agglomeration and the attendant momentum exchange due to the collision and exchange of momentum between size bins due to a change in size, and drag upon a droplet by the continuous phase, i.e. $s_{momentum}^i = s_{aggmomentum}^i + s_{drag}^i$. The transfer of momentum due to droplet agglomeration is

$$s_{aggmomentum}^i = s_{agg} \mathbf{v}_d^i \quad (18)$$

where s_{agg} is the source term described earlier in this section.

The term that represents the drag on the droplet by the continuous phase is

$$s_{drag}^i = \frac{1}{2} C_D \rho_g \pi D_i^2 \| \mathbf{v}_g - \mathbf{v}_d^i \| (\mathbf{v}_g - \mathbf{v}_d^i) \quad (19)$$

where ρ_g is the density of the continuous, gas phase, D_i is the diameter of the droplets in bin i , and C_D is the coefficient of drag.

3. CROSSFLOW SINGLET OXYGEN GENERATOR

The crossflow singlet oxygen generator is so named because the working fluids travel largely perpendicular to one another. In each of the two geometries considered in this work, the gas, a mixture of He and Cl_2 , enters from the left and exits to the right with oxygen as an additional component. The BHP is sprayed in from the top in two stages. Figure 2 illustrates the two geometries for which sample results will be presented, which we identify as SOG1 and SOG2. They are identical in width and the spray stages in SOG1 and SOG2 are equal in size. The height of the reactor varies by a factor of two from SOG1 to SOG2. The models are two-dimensional.

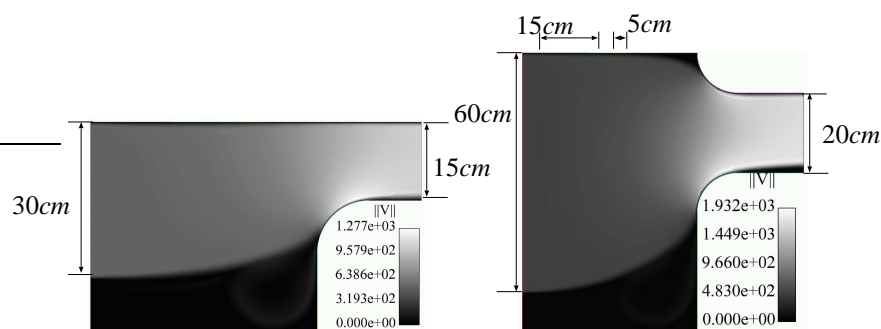


Figure 2. Two 2D geometric configurations of the singlet oxygen generator considered in this paper. The gas phase flows left-to-right, while the droplets primarily convect top-to-bottom.

The boundary conditions of the full SOG model are numerous, but mostly straightforward. At the gas inlet, a uniform velocity profile is prescribed along with the gas composition; see Figure 3. At the exit, a zero vertical velocity and vanishing normal velocity gradient are prescribed. For each geometry, a base case gas velocity of 500 cm/s is specified giving SOG2 twice the volumetric flowrate of gas as SOG1. On all other boundaries, a no-slip and no-penetration boundary conditions are specified for the gas phase.

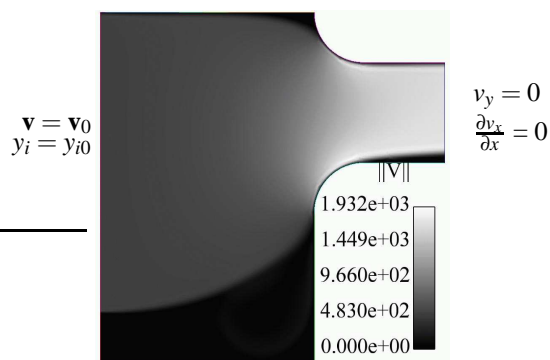


Figure 3. Continuous (gas) phase boundary conditions are no slip and no penetration on all boundaries except inflow and outflow. On the inflow, both geometries introduce gas at 500 cm/s. At the outflow, no vertical velocity and vanishing normal gradient are prescribed.

The liquid phase is sprayed into the reactor in two stages on the top of the reactor, Figure 4. There are three boundary conditions on the liquid phase to be prescribed here. First, the mass fraction of HO_2^- present in the liquid must be specified. The examples assume a 7M mixture of BHP. Second, the distribution of droplet sizes must be specified. This is usually specified as a log-normal distribution. In our sample calculations, the droplet sizes span $200\mu m$ to $2mm$ in diameter with a mean droplet size equal to $300\mu m$. Finally, the velocity of the droplets must be prescribed. In SOG1, the droplet velocity at the inlet is set equal to 500 cm/s for all droplet sizes. Because the gas flowrate of SOG2 is double that of SOG1, the flowrate of liquid in SOG2 is doubled in order to keep the loadings equal, and so the droplet velocity is set equal to 1000 cm/s for all droplet sizes in SOG2.

Droplets are not allowed to penetrate the gas inlet, and so both the number density and droplet velocity are set to zero there. On all other walls, natural boundary conditions are used, so the droplets are simply allowed to penetrate and exit the system. In the case of the gas exit, this captures the effect of droplets becoming entrained and being convected downstream by the gas. On solid walls, this captures the effect of the liquid pooling on walls and draining.

4. RESULTS

For the purpose of studying the performance of the SOG over ranges of parameter space, a base case and evaluation metrics must be chosen. The point of departure, or base case, in this study was mostly described in the preceding section.

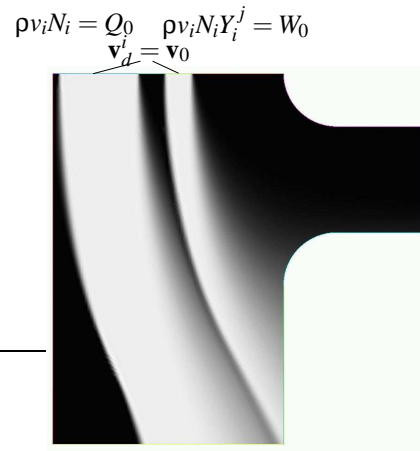


Figure 4. Dispersed (liquid droplets) phase boundary conditions prescribe velocity, composition, and droplet size distribution at the inflow; elsewhere, droplets are allowed to penetrate or coalesce on the wall.

A uniform inlet gas velocity is prescribed at 500 cm/s for both SOG1 and SOG2. Also in both configurations, the inlet gas composition is set equal to 82% He by mole and 18% Cl_2 by mole. The droplet velocity is 500 cm/s in SOG1, 1000 cm/s in SOG2 and an identical droplet size distribution and liquid composition is specified for both.

Evaluation metrics used in this study are common ones in reactor analysis. There is confusion in the names of them, however. The authors defer to the spectrometrists' naming convention but include the more traditional chemical engineering names parenthetically. The first of the metrics is utilization (conversion),

$$u = 1 - \frac{[Cl_2]_o}{[Cl_2]_i} \quad (20)$$

where $[\]$ indicates the concentration of the indicated component and the subscripts i and o indicate that the concentration is to be evaluated at the inflow or outflow, respectively. The other two metrics are yield (selectivity),

$$Y = \frac{[O_2(^1\Delta)]_o}{[O_2(^3\Sigma)]_o + [O_2(^1\Delta)]_o} \quad (21)$$

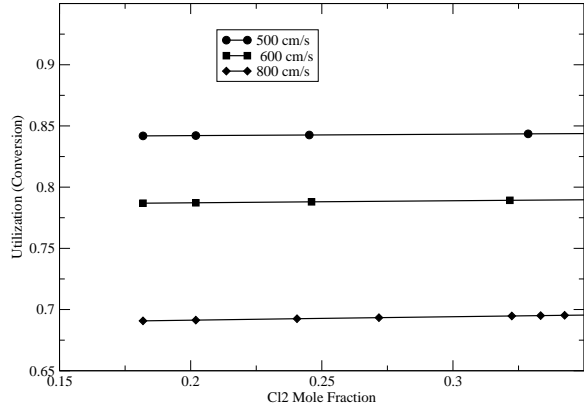
and efficiency (yield)

$$\eta = \frac{[O_2(^1\Delta)]_o}{[Cl_2]_i}. \quad (22)$$

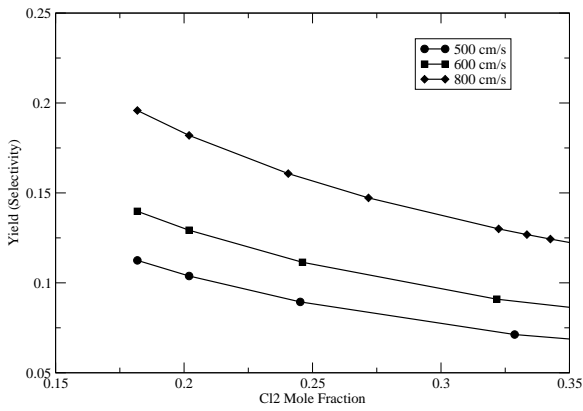
Figure 5 shows the effect of increased gas velocity in SOG1 on all the metrics at a pressure of $P_{SOG} = 78$ Torr and for different gas velocities. Utilization (conversion), seen in Figure 5(a), improves slightly over the range of Cl_2 concentration but diminishes with increased velocity. The reason, simply, is residence time. The higher velocity gas spends less time in contact with the droplets where all conversion occurs. Yield (selectivity) and efficiency (yield), seen in Figures 5(b) and 5(c), show different trends. All three diminish with Cl_2 concentration. The reason is because the increased concentration of Cl_2 produces a greater concentration of $O_2(^1\Delta)$. The greater concentration of $O_2(^1\Delta)$ increases the loss path by pool quenching; see the reaction in Equation 7. These figures of merit improve with gas velocity. The reason again is residence time. Less time in the reactor means less time for quenching to occur.

As can be seen in Figure 6, which was computed at 500 cm/s gas velocity and a pressure of 78 Torr, the drag on the droplets is approaching the level to be sufficient to entrain the smallest of the droplets into the gas exit stream. Because of the detrimental effect of entrained droplets on the performance and equipment in the lasing section of the COIL, these operating conditions are to be avoided.

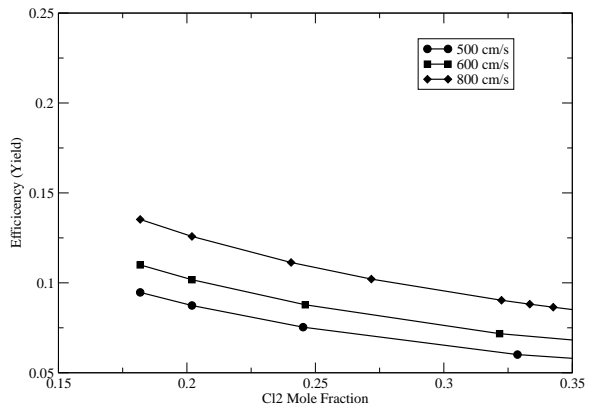
Figures 7(a) and 7(b) show all three metrics in a SOG1 versus SOG2 comparison. Figure 7(a) shows the effect of pressure and Figure 7(b) the effect of Cl_2 . In both cases, as before, the increased $O_2(^1\Delta)$ concentration that results from increased Cl_2 concentration due to greater pressure or mole fraction leads to greater pool quenching and reduced efficiency



(a) SOG1 Utilization (Conversion)



(b) SOG1 Yield (Selectivity)



(c) SOG1 Efficiency (Yield)

Figure 5. Performance of SOG1 as the gas velocity increases from 500 cm/s to 1200 cm/s.



(a) 200 μm droplets

(b) 300 μm droplets

(c) 400 μm droplets

Figure 6. Flow field of droplets in the SOG. These represent the three smallest droplet bins. This illustrates how the smaller droplets are more strongly entrained by the gas.

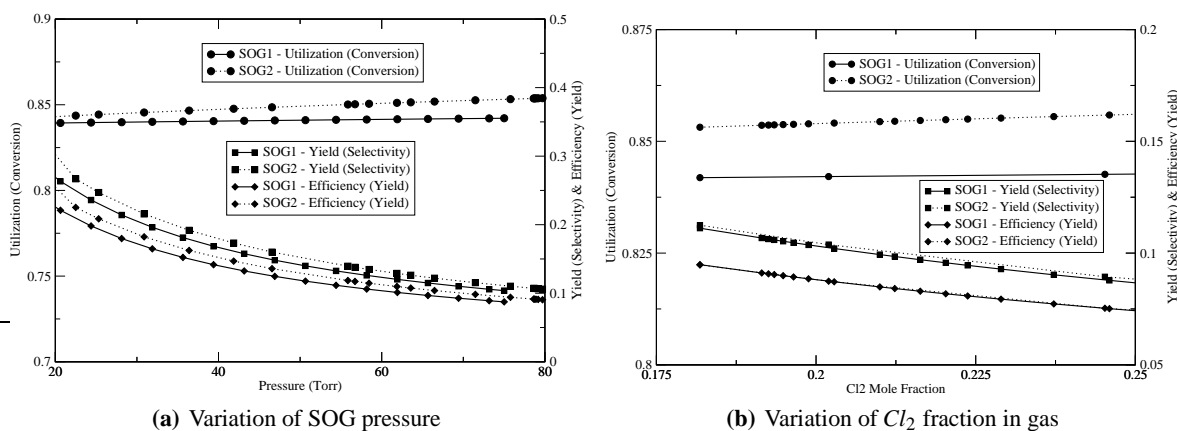


Figure 7. Utilization (conversion), yield (selectivity) and efficiency (yield) of SOG1 and SOG2 given variation in reactor pressure and inlet gas stream composition.

and yield. There is very little advantage to either SOG configuration apparent from these data. Though it is certain that SOG2 produces a greater quantity of O_2 ($^1\Delta$) because of the increased flowrates.

Figure 7(b) shows the effect of the inlet gas composition by increasing the fraction of Cl_2 from 18% to 22% by mole. This study was completed at one of the higher pressures studied of 78 Torr. Once again, SOG1's performance trends downward as the fraction of Cl_2 is increased and SOG2 appears to be largely unaffected by the composition over the ranges studied.

5. CONCLUSIONS

This study demonstrates the possibilities of using multiphase flow models and large-scale computing resources to study singlet oxygen generator designs. With this approach, investigations covering a wide range of parameter space can undertaken. It also shows that the geometrical configuration of the reactor can be studied easily by mathematical manipulation of boundaries—a decided economical edge over the construction of many experimental apparatus.

Acknowledgments

Sandia is a multiprogram laboratory operated by Sandia Corporation, a Lockheed-Martin Company, for the United States Department of Energy under contract DE-AC04-94AL85000.

REFERENCES

- [1] Shadid, J., Salinger, A. G., Pawlowski, R. P., Lin, P. T., Hennigan, G. L., Tuminaro, R., and Lehoucq, R. B., "Large-scale stabilized fe computational analysis of nonlinear steady state transport / reaction systems," *Comp. Meth. in App. Mechanics and Eng.* **195**, 1846–1876 (2006).
- [2] Musson, L. C., Hill, J. H., Pawlowski, R. P., and Salinger, A. G., "Theoretical modeling of multiphase, reacting high speed flows in singlet oxygen generators," *Manuscript in preparation*.
- [3] Thayer III, W. J., Cousins, A. K., and Romea, R. D., "Modeling of uniform droplet singlet oxygen generators," *Proceedings of the SPIE* **2117**, 71–100 (1994).
- [4] Gelbard, F. and Seinfeld, J. H., "Simulation of multicomponent aerosol dynamics," *Journal of Colloid and Interface Science* **78**(2), 485–501 (1980).